

# Hydrogen Influence on Fatigue Crack Paths in 25 Cr 7 Ni Superduplex Stainless Steel

V. Di Cocco<sup>1</sup>, E. Franzese<sup>2</sup>, F. Iacoviello<sup>1</sup>, S.Natali<sup>2</sup>

<sup>1</sup> Università di Cassino, Di.M.S.A.T., via G. Di Biasio 43, Cassino (FR), Italy, iacoviello@unicas.it

<sup>2</sup> Università di Roma “La Sapienza”, I.C.M.M.P.M., via Eudossiana 18, Roma, Italy

**ABSTRACT.** Duplex stainless steels (DSSs) fatigue crack propagation resistance is strongly affected both by microstructure and environment. In this work, environment influence on the fatigue crack propagation in a rolled 25 Cr 7 Ni superduplex stainless steel was investigated considering three different stress ratios ( $R = K_{min}/K_{max} = 0.1, 0.5, 0.75$ ). Tests were performed according to ASTM E 647 standard, both in air and under hydrogen charging conditions ( $0.1M H_2SO_4 + 0.01 M KSCN$  aqueous solution,  $-0.9 V/SCE$ ). Crack fracture surfaces were extensively analysed by means of a scanning electron microscope. Furthermore, crack paths were investigated by means of a crack profile analysis. Nickel coated fracture surface sections obtained for constant  $\Delta K$  values were considered in order to analyse the loading condition influence ( $R$  values and environment) on fatigue crack paths.

## INTRODUCTION

Duplex stainless steels are successfully used in chemical, petrochemical, nuclear, fertilizer and food industries, due to their good mechanical properties and their excellent generalized and localized corrosion resistance, in many environments and operating conditions, like chloride induced stress corrosion [1, 2]. Depending on their chemical composition, these steels are prone to age hardening and embrittlement over a wide temperature range. This is mainly due to precipitation phenomena that may occur inside ferrite grains and at ferrite-austenite grain boundaries [3, 4].

In order to analyse the influence of hydrogenating environments on stainless steels mechanical behaviour, many factors should be taken into account; environment, surface and metallurgical conditions and hydrogen physical behaviour are only the main factors that influence the complex problem of hydrogen embrittlement. In aqueous solutions, the analysis of fatigue crack propagation resistance under hydrogen charging conditions could be considered as characterized by five different stages [5]:

1. Electrochemical mass transport;
2. Anodic and cathodic surface reactions;
3. Hydrogen absorption reactions;
4. Hydrogen transport and trapping;
5. Hydrogen embrittlement.

Considering all the physical, chemical, metallurgical and mechanical parameters that influence the hydrogen charging, diffusion, solubility and trapping in metals, many hydrogen embrittlement models are available, but no one is applicable to all the possible conditions. Among them, it is possible to remember [6, 7]:

- Models based on the hydrogen internal pressure, connected to the molecular hydrogen recombination corresponding to microvoids or interfaces, with a consequent crack growing due to the high hydrogen pressures.
- Models based on the surface energy decreasing, due to the adsorbed hydrogen presence, with a consequent embrittlement increasing.
- Models based on the cohesion decreasing, where the hydrogen presence implies a decrease of the interatomic cohesion at the crack tip;
- Models based on the interaction of hydrogen and plastic deformation: they are based on the complex interactions between hydrogen and dislocations during the plastic deformation (plastic deformation influences hydrogen diffusion and trapping and, considering very slow strain rate values, hydrogen follows the dislocations displacement, modifying the mechanical behaviour)
- Models based on the hydrides precipitation or fragile phases formation (e.g. formation of  $\alpha'$ , cc, or  $\epsilon$ , hc, martensitic phases in metastable austenitic stainless steels that could be hydrogen induced).
- Hydrogen assisted fatigue crack propagation is characterised by some peculiarities with respect to the hydrogen embrittlement mechanisms formerly shown (e.g., the influence of mechanical parameters such as loading frequency or stress ratio).

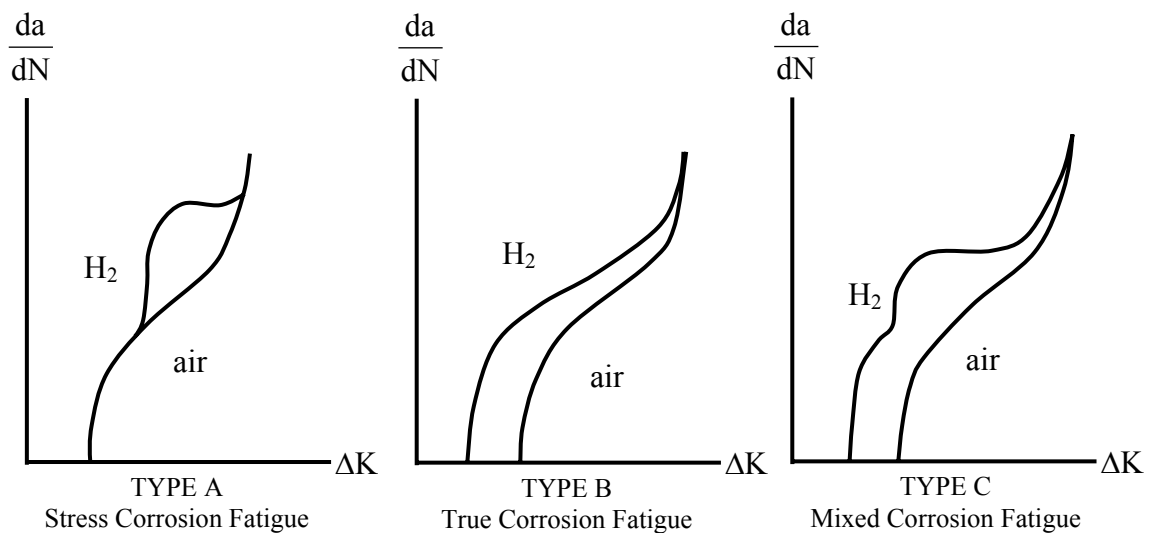


Figure 1. Classifications of corrosion fatigue [8].

In fact, hydrogen assisted corrosion fatigue main behaviours could be classified as follows (Fig. 1):

- Stress corrosion fatigue (type A), where a sharp increase in fatigue crack growth is observed, corresponding to a critical stress intensity, with respect to the inert environment behaviour; this is due to the superposition of the pure fatigue crack growth with a time dependent stress corrosion cracking;
- True corrosion fatigue (type B), where an evident threshold value  $\Delta K_{th}$  decrease and a crack growth rates increase are observed, without a critical stress intensity value.
- A combination of true corrosion fatigue, for lower  $\Delta K$  values, and stress corrosion fatigue, for higher  $\Delta K$  values (type C).

The aim of this work is the analysis of the fatigue crack propagation resistance of a rolled superduplex stainless steels and the investigation of the microstructure influence on fatigue crack propagation micromechanisms.

## MATERIAL AND EXPERIMENTAL METHODS

Hydrogen influence on fatigue crack propagation resistance of an austeno-ferritic (superduplex) 25 Cr 7 Ni stainless steels was investigated (Table 1).

Table 1. 25 Cr 7 Ni austenitic-ferritic stainless steel chemical composition and tensile properties (T);  $\alpha\% = \gamma\% = 50$

C	Si	Mn	P	S	Cr	Ni	Mo	N
0.019	0.33	0.80	0.020	0.001	24.80	6.80	3.90	0.30
YS [MPa]		UTS [MPa]		$\epsilon_r\%$				
556		814		31				

Fatigue tests were run according to ASTM E647 standard [9], using CT (Compact Type) 10 mm thick specimens and considering three different stress ratio values (e.g.  $R = P_{min}/P_{max} = 0.1; 0.5; 0.75$ ). Tests were performed using a computer controlled Instron 8501 servohydraulic machine in constant load amplitude conditions, considering a 30 Hz loading frequency, a sinusoidal waveform and laboratory conditions. Crack length measurements were performed by means of a compliance method using a double cantilever mouth gage. Tests were performed at room temperature, both in air, with a loading frequency of 30 Hz, and under hydrogen charging conditions (0.5 M  $H_2SO_4$  + 0.01 M KSCN aqueous solution; applied potential = -0.9 V/SCE), with a loading frequency of 1 Hz (Fig. 2).

Fracture surfaces were analysed by means of a scanning electron microscope (SEM). Fatigue crack path analysis was performed considering all the fractured specimens, by means of an optical microscope (x200), according to the following procedure:

- Fracture surface nickel coating (in order to protect fracture surface during cutting);

- Fractured specimen transversal cutting, corresponding to different crack length (applied  $\Delta K$  values = 10, 15, 20  $\text{MPa}\sqrt{\text{m}}$ );
- Metallographic preparation of the section (up to  $0.2 \mu\text{m}$   $\text{Al}_2\text{O}_3$  powder)
- Chemical attack performed in a 10 ml  $\text{HNO}_3$  + 20 ml  $\text{HCl}$  + 30 ml  $\text{H}_2\text{O}$  solution for about 15 minutes.

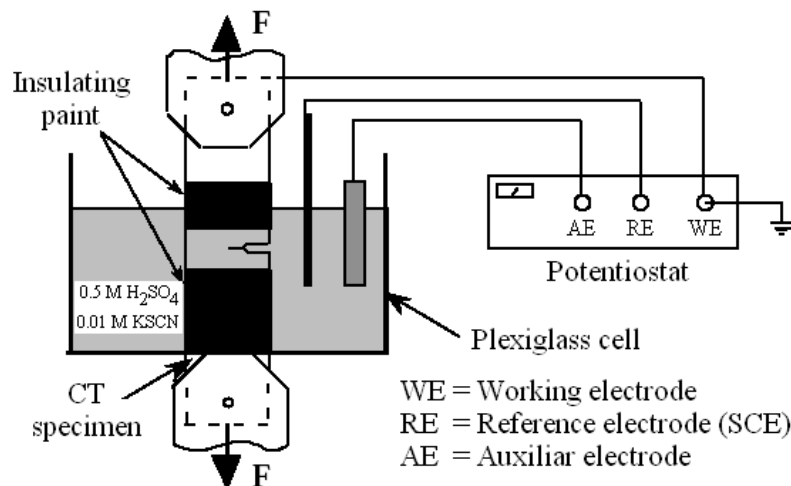


Figure 2. Fatigue crack propagation in hydrogen charging conditions experimental apparatus.

## RESULTS AND DISCUSSION

Stress ratio and loading conditions influence on superduplex fatigue crack propagation resistance is shown in Fig. 3.

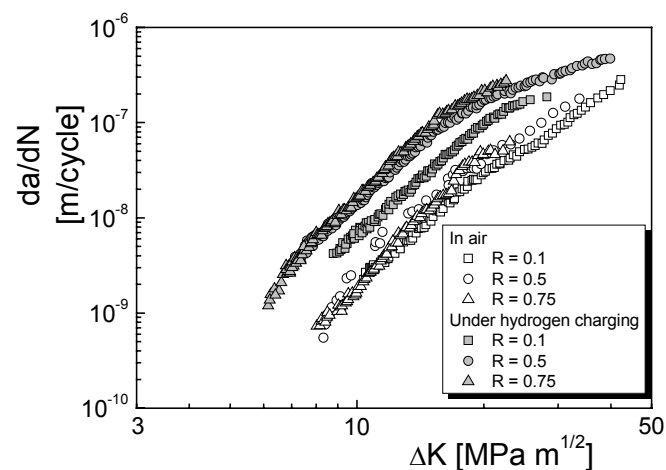


Figure 3. Stress ratio and environment influence on 25 Cr 7 Ni stainless steel fatigue crack propagation resistance.

Considering tests performed in air, stress ratio influence is completely negligible. Hydrogen charging implies an increase of crack growth rate for all the investigated loading conditions (R and  $\Delta K$  values). Higher differences between crack growth rates obtained under hydrogen charging conditions and in air are obtained with higher R values. Corresponding to a crack growth rate under hydrogen charging conditions of about  $2 \cdot 10^{-7}$  m/cycle, differences between crack growth rates obtained under hydrogen charging conditions and in air decrease. SEM fracture surface analysis shows the environment influence on fatigue crack paths (crack growths from left to right, Figs. 4-7).

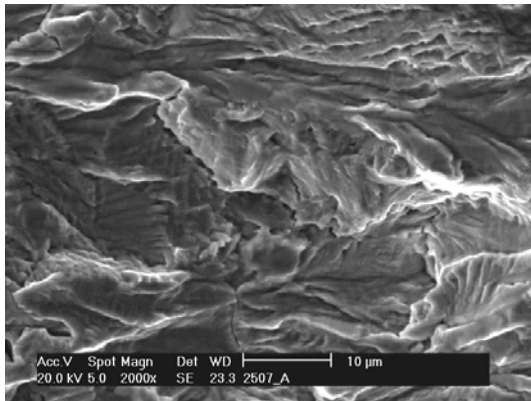


Figure 4. Fatigue crack propagation in air ( $\Delta K = 10 \text{ MPa}\sqrt{\text{m}}$ ,  $R = 0.1$ ).

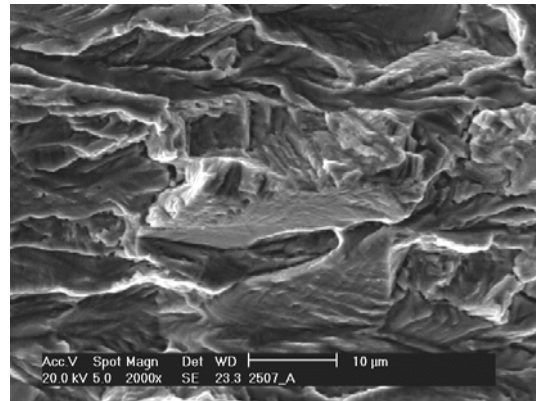


Figure 5. Fatigue crack propagation in air ( $\Delta K = 20 \text{ MPa}\sqrt{\text{m}}$ ,  $R = 0.75$ ).

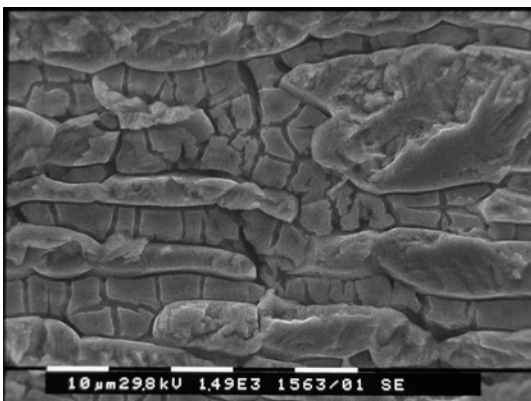


Figure 6. Fatigue crack propagation under hydrogen charging conditions ( $\Delta K = 10 \text{ MPa}\sqrt{\text{m}}$ ,  $R = 0.1$ ).

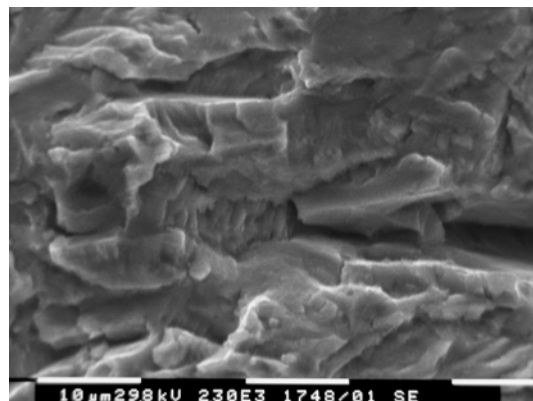


Figure 7. Fatigue crack propagation under hydrogen charging conditions ( $\Delta K = 20 \text{ MPa}\sqrt{\text{m}}$ ,  $R = 0.75$ ).

Fracture surfaces obtained in air are characterized by morphologies that do not depend on R value, but only on the applied  $\Delta K$ . Corresponding to lower applied  $\Delta K$  values (stage I and stage II of crack propagation), fracture surfaces are characterized by ductile morphologies, with the presence of ductile striations (Fig. 4). Higher applied  $\Delta K$  values imply to an increase of the cleavage importance corresponding to ferrite grains

(Fig.5). Under hydrogen charging conditions, ferrite grains cleavage is really evident, especially for lower applied  $\Delta K$  values and lower R values (Fig. 6). Short secondary cracks are present and propagate both in ferrite grains and at  $\alpha/\gamma$  grain boundaries. Higher applied  $\Delta K$  and R values are characterized by the presence of long secondary cracks that start in ferrite grains or at  $\alpha/\gamma$  grain boundaries (Fig. 7).

Crack path transversal profiles were obtained for three different  $\Delta K$  values (respectively 10, 15 and 20  $\text{MPa}\sqrt{\text{m}}$ ,  $R = 0.1$ ), both in air (Fig. 8) and under hydrogen charging conditions (Fig 9): ferrite grains are dark grey and austenite grains are light grey.

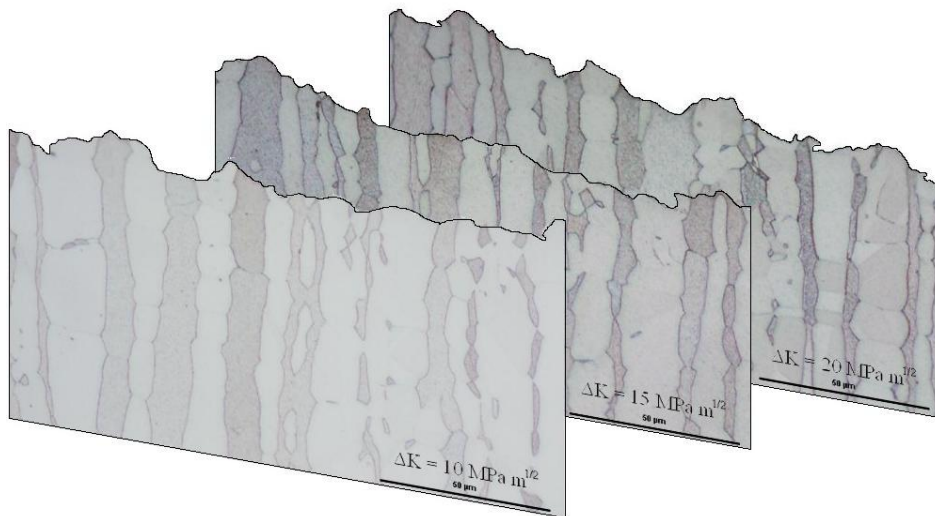


Figure 8. Fatigue crack profiles: test performed in air.

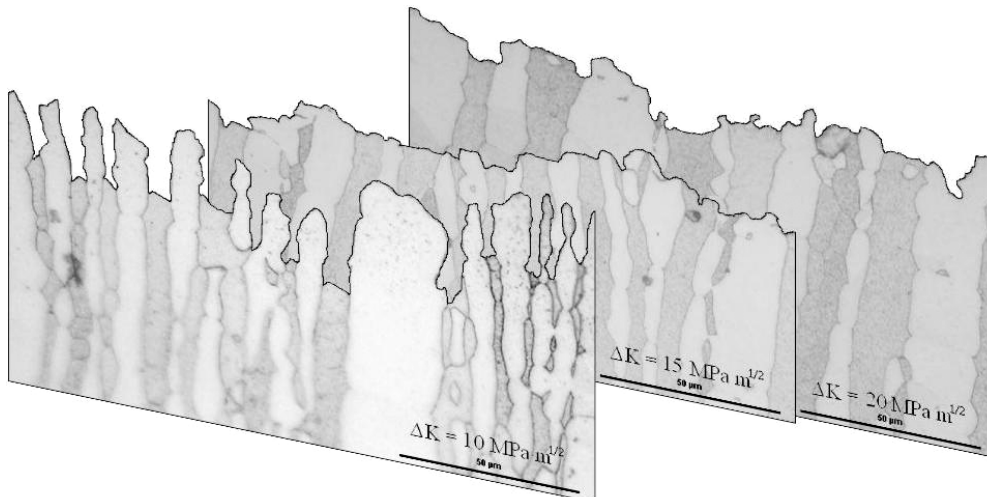


Figure 9. Fatigue crack profiles: test performed under hydrogen charging conditions.

Hydrogen charging during fatigue crack propagation strongly influences fracture surface morphology, especially corresponding to lower  $\Delta K$  values: for these loading conditions, a peculiar crack profile is obtained, with a really evident ferrite grains

cleavage and ductile deformation of austenite grains. The increase of the applied  $\Delta K$  implies a decrease of the austenite grains ductile deformation evidence, with ferrite grains that are still characterized by an evident cleavage. This behaviour is due to the different hydrogen embrittlement susceptibility of austenite and ferrite and to different embrittlement mechanisms. Corresponding to lower  $\Delta K$  values (lower crack growth rates), ferrite grains are deeply hydrogen charged, due to their high diffusion coefficients. As a consequence, a semi-cohesive zone is obtained at the crack tip, with ferrite grains that are characterized by a cleavage fracture and austenite grains that show a transgranular fracture probably caused by the localization of the slip process, with a consequent promotion of dislocations generation/motion [10]. In a range of strain rates, presence of hydrogen in solid solution decreases dislocation motion barriers [11], with a consequent increase of the amount of deformation in a localized region (hydrogen enhanced localized plasticity, HELP, mechanism). Higher applied  $\Delta K$  values imply an increase of crack growth rates. As a consequence, due to their high hydrogen diffusion coefficients and their high hydrogen embrittlement susceptibility, ferrite grains are always hydrogen embrittled (cleavage is evident) and austenite grains are not interested by the HELP mechanism and, due to their low hydrogen diffusion coefficient and to the higher crack growth rates, they are only partially hydrogen charged. As a consequence, fracture surface morphology is similar to the one obtained in air. Macroscopically, this implies lower differences of crack growth rates obtained in air and under hydrogen charging conditions (Fig. 3).

## CONCLUSIONS

In the present work, fatigue crack propagation resistance of a 25 Cr 7 Ni superduplex (austenitic-ferritic) rolled stainless steel was investigated both in air and under hydrogen charging conditions, considering three different stress ratios. SEM fracture surfaces analysis was performed and crack paths were investigated by means of a crack profile analysis. Nickel coated fracture surface sections obtained for constant  $\Delta K$  values were considered in order to analyse the loading condition influence (R values and environment) on fatigue crack paths. On the basis of the experimental results, the following conclusions can be summarized:

- for all the investigated loading conditions (R and  $\Delta K$  values), superduplex stainless steel hydrogen embrittlement is evident; differences between fatigue crack growth rates obtained in air and under hydrogen charging conditions are less evident corresponding to higher applied  $\Delta K$  values;
- SEM fracture surface analysis shows a strong hydrogen influence on fracture morphology, with the presence of an evident ferrite grains cleavage, transversal secondary (lower  $\Delta K$  values) and longitudinal secondary cracks (higher  $\Delta K$  values);
- Crack profile analysis allowed to evidence the peculiar fracture morphology obtained under hydrogen charging conditions (lower  $\Delta K$  values), probably due to the hydrogen enhanced localized plasticity, HELP, mechanism.

## REFERENCES

1. Lacombe, P. Baroux, B. Beranger, G. (1990) *Les aciers inoxydables*, Les éditions de physique, Les Ulis Cedex A, France 663-682.
2. Dupouiron, F. Aoudouard, J. P. (1996) *Scand. J. Mater.* **25**, 95.
3. Charles, J. (2000) *Duplex 2000 6<sup>th</sup> World*, Venice, Italy 1-42.
4. Iacoviello, F. Casari, F. Gialanella, S. (2005) *Corrosion Science*, **47**, 909-922.
5. Thomas, J.P. Chopin, C.E. (1994) *Fifth International conference on the hydrogen effect in materials*, edited by A.W. Thompson and N. R. Moody, 233-242.
6. Coudreuse, L. (1990) *Corrosion sous contrainte*, edited by D. Desjardins and R. Oltra, Bombannes, 397-424.
7. Carter, T.J. Cornish, L.A. (2001) *Engineering failure analysis*, **8**, 113-121.
8. Marrow, T.J. Hipsley, C.A. King, J.E. (1991) *Acta Metall. Mater.*, **39**, 6, 1367-1376.
9. *ASTM Standard test Method for Measurements of fatigue crack growth rates (E647-93)*, Annual Book of ASTM Standards (1993), vol. 0301, American Society for Testing and Materials.
10. Tsay, L. W. Liu, Y.C., Young, M. C. Lin, D.Y. *Materials Science and Engineering A* 374 (2004), 204-210.
11. Sofronis, P. Liang, Y. Aravas, N. *Eur. J. Mech. A/Solids* 20 (2001), 857-872.